Properties of Electrodeposited Ni-B-ZrO$_2$ Composite Coatings

R. A. Shakoor[1], Ramazan Kahraman[2] ,Umesh S. Waware[2], Yuxin Wang[3], Wei Gao[3]*

[1] Center for Advanced Materials, Qatar University, P. O. Box 2713, Doha, Qatar
[2] Department of Chemical Engineering, College of Engineering, Qatar University, P. O. Box 2713, Doha, Qatar
[3] Department of Chemical and Materials Engineering, The University of Auckland, Private Bag 92019, Auckland 1142, New Zealand.
[*]E-mail: ramazank@qu.edu.qa

Ni-B coatings have high hardness and high wear resistance which make them suitable for automotive, aerospace, petrochemical, textile and electronics industries. Further improvement in properties (especially the corrosion behavior) will extend their range of applications and thus make them suitable to high wear and severe corrosion applications of oil and gas industries. Taking a note of above consideration, novel Ni-B-ZrO$_2$ coatings were synthesized. In the present study, a comparison of properties of Ni-B and Ni-B-ZrO$_2$ coatings in their as deposited state is presented to elucidate the effect of ZrO$_2$ addition on structural, surface, thermal and electrochemical properties of binary Ni-B coatings. Mild steel samples were used as substrate material and the coatings were deposited through conventional electrodeposition process using dimethylamine borane (DMAB) as reducing agent. It is noticed that the addition of ZrO$_2$ has a significant influence on crystal structure, surface roughness, thermal properties and corrosion behavior Ni-B coatings. It is noticed that Ni-B coatings are amorphous in their as deposited state while addition of ZrO$_2$ significantly improves the crystallinity. Surface analyses confirm the formation of fine and dense structures in both Ni-B and Ni-B-ZrO$_2$ coatings. However ZrO$_2$ addition increases the surface roughness. The electrochemical polarization tests confirm that incorporation of ZrO$_2$ into Ni-B matrix considerably improves the corrosion resistance due to reduction in active area of Ni-B matrix.

1. INTRODUCTION

The components in industrial plants are subjected to high corrosion and wear. Owing to these deleterious processes, the gradual deterioration of metallic surfaces occurs which usually reduces the plant production and sometimes a shutdown. The combined effects of wear and corrosion cause much

higher material loss that can be caused by the each process happened separately. Corrosion and wear may cause severe damages and safety issues in a number of industries which are not limited to only process and manufacturing industries[1]. Presently, metal deposition processes using aqueous solutions (electrodepositon and electroless plating) are getting substantial attention owing to their remarkable advantages such as simplicity, economy, high deposition rate, uniformity of the deposit, decent wear and corrosion properties. Both electroless and electrodeposition processes have been adopted to deposit Ni-B coatings. Ni-B coatings possess very attractive properties like high hardness), high wear resistance (better than hard chromium coatings) and decent anti-corrosion properties (Ni-P coatings). In addition, many other amazing characteristics of Ni–B coating such as cost-effectiveness, thickness uniformity, lubricity, good ductility, excellent solderability, good electrical properties, antibacterial property, low porosity, superior bonding and extraordinary electromagnetic properties have also been recognized. Owing to their tempting properties, Ni-B coatings are finding their applications in automotive, aerospace, nuclear, petrochemical, computer, electronics, plastic, optics, textile, paper, food and printing industries [2].

Different types of substrates have been used to deposit electroless Ni-B coatings which mainly include mild steel, stainless steel, aluminum, copper and magnesium alloys. During this process, both dimethylamine borane (DMAB) and sodium borohydride have been successfully employed as reducing agents [1, 3, 4]. At the same time, electrodeposition process is quite popular to synthesize coatings of a wide variety of materials including nano composites. Electrodepositon of Ni-B coatings have been accomplished by use of a different reducing agents such as sodium borohydride[4], dimethylamine borane[5, 6], trimethylamine borane[7], carborane ion[8] and sodium decahydroclovodecaborate[8, 9]. The obvious advantages of electrodeposition includes; low cost, low porosity, high purity, large production rate, no shape limitations, higher deposition rates, use of a range of substrates, good composition control and development of some unique types of coatings [8, 10]. In spite of these apparent advantages, electrodeposition process has not yet been frequently adopted to synthesize Ni-B coatings.

Among various reinforcement choices, ZrO_2 was selected due to its encouraging effect on structural, mechanical and corrosion resistance properties when added to Ni and Ni-P coatings [11-15]. Furthermore, the effect of ZrO_2 addition on properties of binary Ni-B coatings has not yet been investigated. By considering the heartening role of ZrO_2 addition, we have developed novel Ni-B-ZrO_2 composite coatings through conventional electrodeposition process.

In the present study, the effect of ZrO_2 addition on structure, surface morphology, thermal properties and corrosion behavior of Ni-B coatings is presented to elucidate the beneficial role of ZrO_2 addition to binary Ni-B coatings.

2. EXPERIMENTAL DETAILS

Ni-B and Ni-B-ZrO_2 composite coatings were electrodeposited on low carbon steel substrates having size diameter 20 X 5 mm. The compositional analysis of mild steel used as substrate is presented in Table 1. All substrates were mechanically cleaned from corrosion products prior to the

coating process. During the process of mechanical cleaning, the substrates were gradually cleaned up to 1200 SiC paper. After mechanical cleaning, degreasing of all the samples was under taken with acetone. The samples were then cleaned in an alkaline solution and thoroughly washed with distilled water. Finally, the surfaces of all the above prepared substrates were activated with a 20 % solution of HCl for about 1 minute and then thoroughly washed with distilled water. The solution bath composition and parameters adopted for electrodeposition of Ni-B and Ni-B-ZrO$_2$ coatings are presented in Table 2. Pure nickel plate was employed as anode and low carbon steel substrate was used as cathode. The coatings deposition was conducted at 43±1˚C for a time period of 60 minutes. During the coating process, the vigorous agitation of the solution was maintained to have uniform deposition and prevention of precipitation of ZrO$_2$ particles. The Ni-B-ZrO$_2$ coatings were synthesized by adding ZrO$_2$ powdered particles into the above mentioned Ni-B coating solution. The chemical composition of the synthesized coatings was determined with ICP-AES (Thermo, iCAP 6500, USA) and EDX analyses. X-Ray diffraction (XRD) analysis was carried out to check the phase purity and structure of the synthesized coatings. X-Ray diffractometer (Rigaku, Miniflex2 Desktop, Tokyo, Japan) equipped with Cu Kα radiations. The analysis of surface and particle morphology of the coatings was determined with the help of field emission scanning electron microscope (FE-SEM-Nova Nano-450, Netherland) and atomic force microscopy (AFM-USA). The AFM device MFP-3D Asylum research (USA) equipped with a Silicon probe (Al reflex coated Veeco model– OLTESPA, Olympus; spring constant: 2 N m^{-1}, resonant frequency: 70 kHz) was used in our experiments. The phase transformation in the coatings was studied with differential scanning calorimetry (DSC, JADE, Perkin Elmer). The scans were conducted from room temperature to 450 ˚C using argon as protective medium. The corrosion behavior of electrodeposited Ni-B and Ni-B-ZrO$_2$ composite coatings in as deposited states was evaluated at room temperature by linear polarization using a Potentiostat/Galavanstat (Autolab, AUT85308, Netherlands). The linear polarization scans were conducted in 3.5 % NaCl aqueous solution.

Table 1. Compositional analysis of steel substrate.

C (Wt.%)	Si (Wt.%)	Mn (Wt.%)	P (Wt.%)	S (Wt.%)
0.186	0.214	0.418	0.029	0.019

Table 2. Solution composition and operating conditions for electrodeposited coating bath.

Sr.#	Chemicals	Composition
1	Nickel sulphate hexa hydrate	240g/l
2	Nickel chloride hexa hydrate	45g/l
3	Boric acid	30g/l
4	Dimethylamine borane complex	3g/l
5	Zirconium dioxide powder	0 and15 g/l
Operating conditions		

1	pH	4
2	Temperature	43±1˚C
3	Deposition time	60 minutes
4	Current density	50 mA/cm^2
5	Bath agitation	500 rpm

3. RESULTS AND DISCUSSION

During nickel electrodeposition process, the addition of dimethylamine borane complex (BH$_3$NH(CH$_3$)$_2$) and insoluble second phase particles like zirconium dioxide (ZrO$_2$) into solution bath results in co-deposition of boron (B) and zirconium dioxide (ZrO$_2$). Table 3 presents the compositional analysis of Ni-B and Ni-B-ZrO$_2$ composite coatings. It is noticed that both boron (B) and zirconium dioxide (ZrO$_2$) have been successfully co-deposited with nickel forming Ni-B and Ni-B-ZrO$_2$ composite coatings on the surface of the steel substrate. Furthermore, the addition of ZrO$_2$ into Ni-B coatings alters the luster and chemical composition. These findings are consistent with previous studies [16,17].

The incorporation of ZrO$_2$ into electrodeposited Ni-B matrix can be explained on the basis of Guglielmi's model. This model describes that the first step is the adsorption of nickel ions on the surface of ZrO$_2$ particles. In next stage, the diffusion of adsorbed particles towards cathode with their "ionic cloud" takes place through the diffusion layer. Loose adsorption of ZrO$_2$ particles occurs subsequently on the surface of the cathode. Finally, when nickel ions are discharged at the cathode, the ZrO$_2$ particles are encapsulated and get incorporated into the Ni-B matrix [18].

Table 3. Compositional analysis of Ni-B and Ni-B-ZrO$_2$ composite coatings.

Coatings	Ni (Wt.%)	B (Wt.%)	ZrO$_2$ (Wt.%)
Ni-B	92.339	7.661	-
Ni-B-ZrO$_2$	90.810	1.952	7.238

Fig. 1(a) shows the comparison of XRD spectra of substrate, Ni-B and Ni-B-ZrO$_2$ composite coatings in their as deposited states. The same XRD pattern on small 2θ range (40-60) is also presented for clarity purpose in Fig. 1(b). It is noticed that Ni-B coating exhibits a single broad peak as clearly shown in Fig. 1(b). The presence of single broad Ni (111) peak shows amorphous structure of synthesized coatings in their as deposited state. Generally, coatings show amorphous structure if boron contents are more than 4.0 wt.% [19]. The presence of single broad peak in our Ni-B XRD pattern is well consistent with our ICP analysis and the previous studies [20, 21, 22,23]. If the boron contents are more than 8 at. %, the broadening of peak (111) is observed at the cost other peaks [24]. However, unlike Ni-B coating, XRD pattern of Ni-B-ZrO$_2$ composite coating exhibits sharp peaks which explain

the crystalline nature of the composite coating. This result suggests that incorporation of ZrO_2 particles has caused significant changes in the structure of Ni-B coatings. The addition of second phase particles into Ni-B coatings usually result in alteration of metallic luster, surface roughness and composition which effect their structural, mechanical and electrochemical properties[17]. Therefore, by comparing our results with Ni-B coatings, it can be noticed that the inclusion of ZrO_2 particles into Ni-B matrix has resulted in structural transformation and thus improves intensities of peaks of Ni (111), Ni (200), Ni (220), Ni (311) and Ni (222).
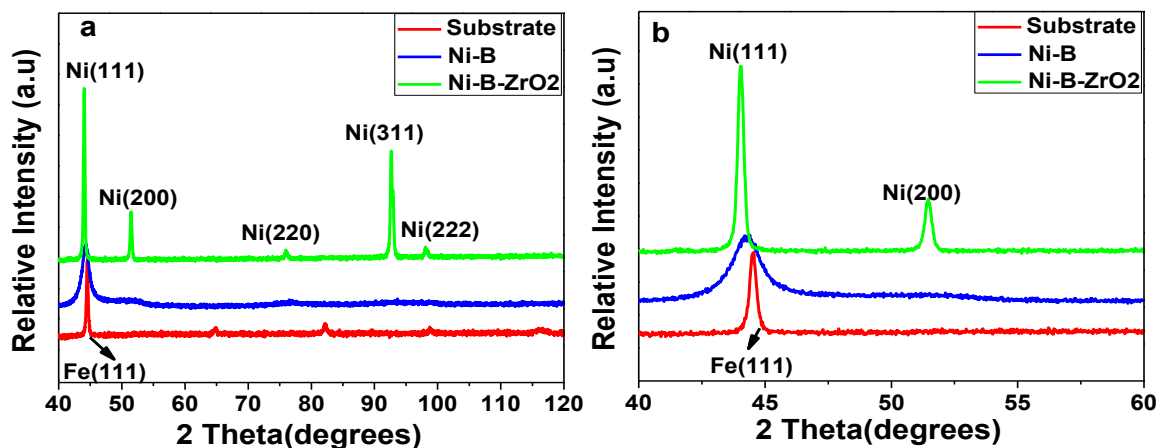
Figure 1. Comparison of XRD spectra of Ni-B and Ni-B-ZrO_2 composite coatings in their as deposited states.

The surface morphology of Ni-B and Ni-B-ZrO_2 composite coating in their as deposited states is presented in Fig. 2. The comparison of SEM images indicates that Ni-B coatings and -B-ZrO_2 composite consist of uniform, fine grained and dense deposits (Fig. 2 (a, b)). The uniform distribution of ZrO_2 particles throughout the matrix is quite visible (Fig. 2 (b)).The fine surface morphology of Ni-B-ZrO_2 composite coatings can be regarded as the effect of increase in electro crystalline potential and hindrance of grain growth of newly formed particles due to the presence of ZrO_2 particles [25].
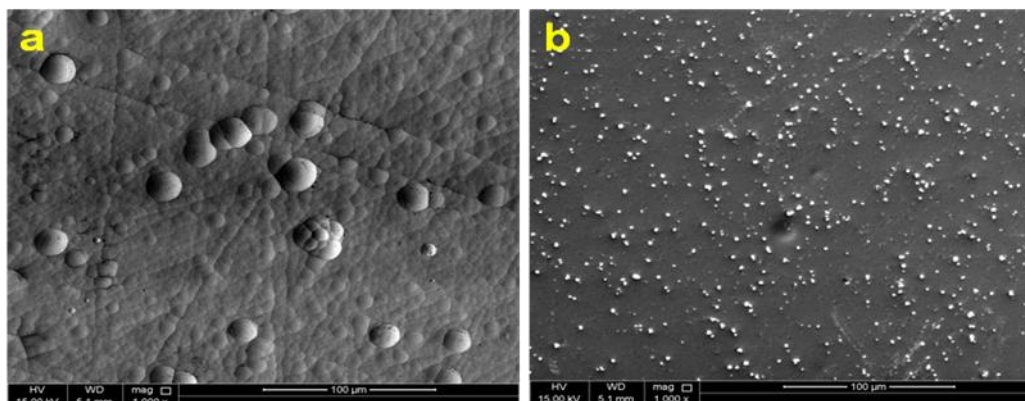

Figure 2. SEM images of synthesized coatings (a) Ni-B and (b) Ni-B-ZrO_2 composite coatings

The EDX spectra of Ni-B and Ni-B-ZrO$_2$ composite coatings are presented in Fig. 3 (a, b). The presence of Ni and B is quite clear as shown in Fig. 3 (a). Furthermore, in addition to Ni and B peaks, the peaks of zirconium have also appeared in the EDX pattern as shown in Fig. 3 (b) which also confirms the co-deposition of ZrO$_2$ particles into Ni-B matrix. The EDX investigation of Ni-B-ZrO$_2$ is consistent with the previous studies related to electrodeposited Ni-B-Si$_3$N$_4$ composite coating[18].
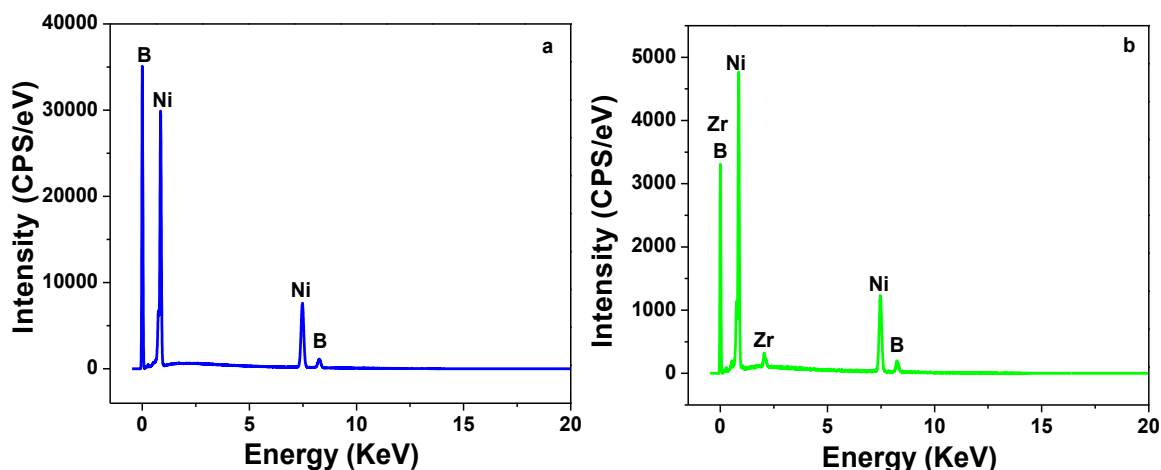

Figure 3. EDX analysis of electrodeposited coatings (a) Ni-B and (b) Ni-B-ZrO$_2$
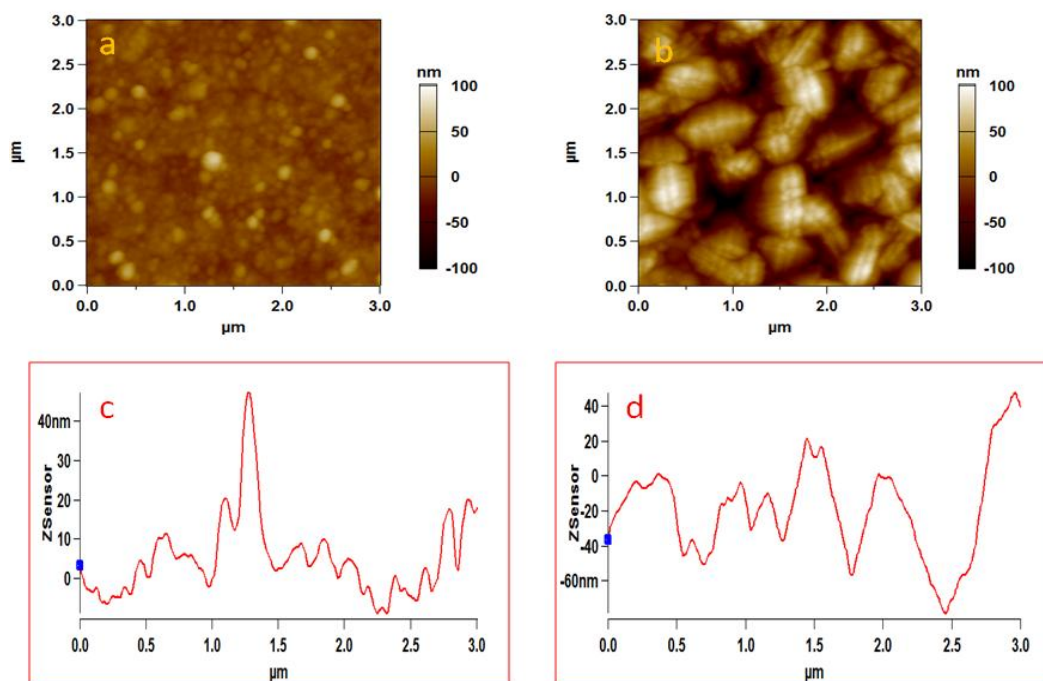
Figure 4. AFM images and corresponding surface profiles of synthesized coatings in as electrodeposited sate; (a) Ni-B coatings (b) Ni-B-ZrO$_2$ alloy coatings (c) surface roughness profile
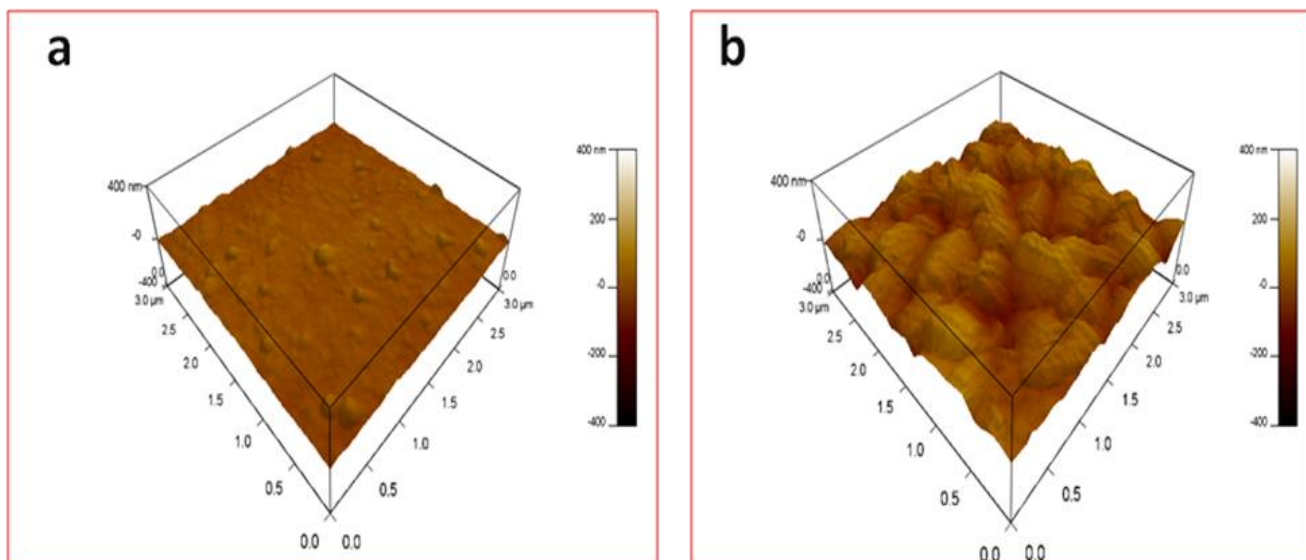
Figure 5. 3-D AFM images of synthesized coatings; (a) Ni-B and Ni-B-ZrO$_2$ alloy coatings in as electrodeposited state.

In order to have deep insight of the surface morphology of the synthesized coatings, the atomic force microscopy (AFM) of the coatings was carried out. The AFM images of Ni-B and Ni-B- ZrO$_2$ alloy coatings with their corresponding surface roughness profiles are presented in Fig. 4 (a, b, c, d). By comparing the surface roughness profiles of both the coatings, it can be noticed that the surface of Ni-B coatings is quite smooth. The surface roughness varies between (0-40 nm)   and plain. However, the surface of Ni-B-ZrO$_2$ alloy coatings is rough and the surface roughness varies (-30-30 nm) which is high when compared with Ni-B coatings. This result indicates that incorporation of zirconia into Ni-B matrix has resulted in relatively high surface roughness. The 3-D AFM images of Ni-B and Ni-B-ZrO$_2$ alloy coatings presented in Fig. 5 (a, b) clearly reveal that Ni-B coatings have a smooth surface but Ni-B-ZrO$_2$ alloy coatings are not smooth as compared with Ni-B coatings.

The DSC results of Ni-B and Ni-B-ZrO$_2$ composite coatings are illustrated in Fig. 6. For a clear comparison, the DSC scan of steel substrate is also shown. It can be noticed that the substrate material (steel) does not show any phase transformation in the entire studied range of temperature. However, Ni-B and Ni-B-ZrO$_2$ composite coatings show phase transformation with the increase in temperature. The Ni-B coatings exhibit first exothermic peaks located at 320 ˚C and the second phase transformation is observed at 362 ˚C with high amount of heat evolution. These two exothermic peaks correspond to the nucleation of two different phases into the microstructure. However, Ni-B-ZrO$_2$ composite coatings show a single exothermic peak at a temperature of 280 ˚C. The different thermal behavior of both the coatings can be attributed to their different chemical compositions. It is reported that the peaks appeared in DSC scans are remarkably influenced by the composition [26-28].
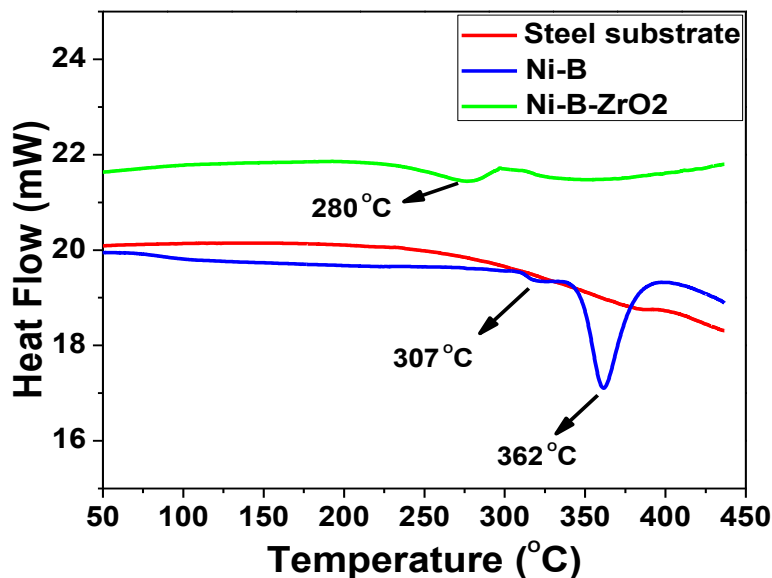
Figure 6. A comparison of DSC scans of steel substrate and electrodeposited Ni-B and Ni-B-ZrO$_2$ composite coatings in their as deposited states.
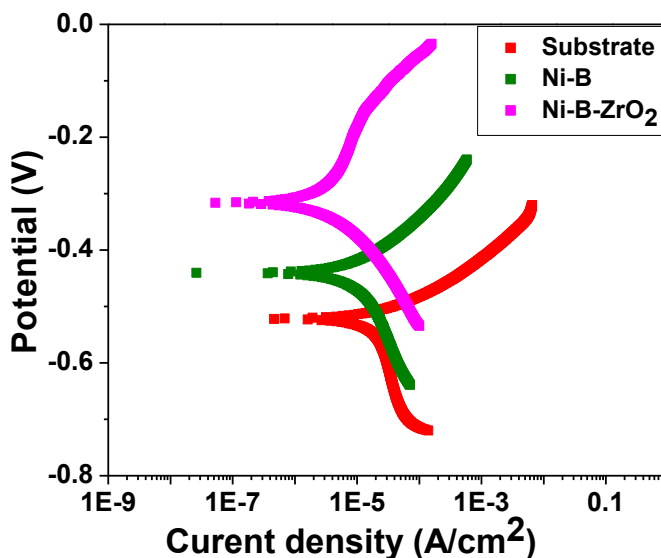

Figure 7. Potentiodynamic Linear polarization curves of (a) steel substrate (b) Ni-B coatings and (c) Ni-B-ZrO2 composite coatings in 3.5 % NaCl aqeous solution.

Potentiodynamic polarization curves for steel substrate, Ni-B and Ni-B-ZrO$_2$ composite coatings are presented in Fig. 7. It can be observed that the addition of ZrO$_2$ particles improves the corrosion properties of Ni-B coatings. This is due to the reason that the values of E$_{corr}$ and I$_{corr}$ of Ni-B-ZrO$_2$ composite coating are more positive as compared to Ni-B coatings and steel substrate. It is also quite clear that Ni-B-ZrO$_2$ composite coatings have higher E$_{corr}$ values and confirms that the addition of ceramic particles like ZrO$_2$ enhances the corrosion confrontation. This improvement in corrosion behavior can be attributed to the reduction in active area of Ni-B matrix which is more prone to

corrode with wetting action of corrosive medium. The effect of ZrO_2 addition in improving corrosion behavior of Ni-B coatings is much pronounced as compared to Si_3N_4 particles[17]. However, the effect of addition of ZrO_2 into Ni-B matrix is found to be similar to its effect when added into Ni-P matrix[29].

4. CONCLUSIONS

It cann be concluded that addition of ZrO_2 into Ni-B matrix has a significant influence on alteraion of chemical composition, crystal structure, surface roughness, thermal properties and corrosion behavior. It is noticed that the addition of ZrO_2 particles to Ni-B matrix enhances crystallinity and surafce roughness. It can also be concuded, inclusion of ZrO_2 into Ni-B matrix results in decent improvement in its corrosion behavior which can be ascribed to reduction in active surafce area of Ni-B matrix by the presence of inactive ZrO_2 particles.

References

1. R.A.Shakoor, R. Kahraman, U. S.Waware, Y.Wang and W. Gao, *Materials and Design.,* 59 (2014) 421.
2. R.A.Shakoor, R. Kahraman, U. S.Waware, Y. Wang, and W. Gao, *Int. J. Electrochem. Sci.,* 9 (2014)5520.
3. R.A. Shakoor, R. Kahraman, W.Gao and Y. Wang, *Int. J. Electrochem. Sci.,* 9 (2014).
4. E.Correa, A.A.Zuleta, L.Guerra, M.A.Gómez, J.G.Castaño, F.Echeverría, H.Liu, P.Skeldon, and G.E.Thompson, *Wear.,* 305 (2013) 115.
5. K.Krishnaveni, TSN.Sankara Narayanan and S.K.Seshadri, *Materials Chemistry & Physics.,* 99 (2006) 300.
6. K.Krishnaveni, TSNS.Narayanan and S.K. Seshadri, *J.Alloys and Compounds.,* 480(2009) 765.
7. K.H.Lee, D. Chang and S.C. Kwon, *Electrochimica Acta.,* 50 (2005)4538.
8. Y.N.Bekish, S.K.Poznyak, L.S.Tsybulskaya and T.V.Gaevskaya, *Electrochimica Acta.,* 55 (2010) 2223.
9. T.V.Gaevskaya and L.S.Tsybulskaya, *Metal Finishing.,* 94 (1996)100.
10. I.B.Gurrappa, *Science and Technology of Advanced Materials.,* 9 (2008)1.
11. K. Zielińska, A. Stankiewicz and I. Szczygieł, *J. Colloid and Interface Science.,* 377 (2012) 362.
12. B. Szczygieł, A. Turkiewicz and J. Serafińczuk, *J. Surface and Coatings Technology.,* 202 (2008) 1904.
13. F. Fernandes, A. Ramalho, A. Loureiro, J.M. Guilemany, M. Torrell and A. Cavaleiro, *Wear.,* 303(2013) 591.
14. Yongjian Yang, Weiwei Chen, Chungen Zhou, Huibin Xu and Wei Gao, *Appl Nanosci.,* 1 (2011)19.

15. W. Wang, F.-Y Hou, H. Wang and   H.-T Guo, *Scripta Materialia.,* 53(2005) 613.
16. K.Krishnaveni, T.S.N.Sankara Narayanan and S.K.Seshadri, *Materials Chemistry and Physics.,* 99 (2006) 300.
17. K.Krishnaveni, T.S.N.S.Narayanan and S.K.Seshadri, *J. Alloys and Compounds.,* 480 (2009) 765.
18. K.Krishnaveni, T.S.N.Sankara Narayanan and S.K Seshadri, *J. Alloys and Compounds.,* 466 (2008) 412.
19. V.Vitry, A.F.Kanta and F.Delaunois, *Materials & Design.,* 39 (2012) 269.
20. K.Krishnaveni, T.S.N.Sankara Narayanan and S.K.Seshadri, *Surface and Coatings Technology.,* 190 (2005) 115.
21. C.T.Dervos, J. Novakovic and P. Vassiliou, *Materials Letters.,* 58(2004)619.
22. Z.A.Hamid, H.B.Hassan and A.M.Attyia, *J. Surface and Coatings Technology.,* 205 (2010) 2348.
23. K.M.Gorbunova, M.V.Ivanov and V.P.Moiseev, *J. Electrochemical Society.,* 120 (1973) 613.
24. Y.N. Bekish, *J.Electrochimica Acta.,* 55 (2010) 2223.
25. N.S.Qu, D.Zhu and K.C.Chan, *Scripta Materialia.,* 54 (2006) 1421.
26. T.S.N.Sankara Narayanan and S.K.Seshadri, *J. Alloys and Compounds.,* 365 (2004) 197.
27. I.Baskaran, *Surface and Coatings Technology.,* 200 (2006) 6888.
28. A.Contreras, *J. Applied Surface Science.,* 253 (2006) 592.
29. Y.W.Song, D.Y.Shan and E.H.Han, *J. Materials and Corrosion.,* 58 (2007) 506.